Electronic Supplementary Information

Photothermal Behaviour of Titanium Nitride Nanoparticles Evaluated by Transient X-ray Diffraction

Benjamin T. Diroll,[a†] Alexandra Brumberg,[b†] Ariel A. Leonard,[b,c] Shobhana Panuganti,[b] Nicolas E. Watkins,[b] Shelby A. Cuthriell,[b] Samantha M. Harvey,[b,d] Eli D. Kinigstein,[e] Jin Yu,[e] Xiaoyi Zhang,[e] Mercouri G. Kanatzidis,[b,d,f] Michael R. Wasielewski,[b,d] Lin X. Chen,[b,c,d] Richard D. Schaller[a,b,d*]*

[a]Center for Nanoscale Materials, Argonne National Laboratory, Lemont, IL 60439

[b]Department of Chemistry, Northwestern University, Evanston, IL 60208

[c]Chemical Science and Engineering, Argonne National Laboratory, Lemont IL 60439

[d]Institute for Sustainability and Energy at Northwestern, Northwestern University, Evanston, IL 60208

[e]X-ray Sciences Division, Argonne National Laboratory, Lemont, IL 60439

[f]Department of Materials Science and Engineering, Northwestern University, Evanston, IL 60208

*bdiroll@anl.gov; schaller@anl.gov

Experimental Details.

Materials. TiN particles were purchased from Plasmachem Gmbh in 20 nm and 50 nm particle sizes. Particles were dispersed in 18 MΩ ultrapure water. When massed by evaporating solvent, solutions were 1.3 (20 nm) and 1.5 (50 nm) mg/mL in in concentration.

Static optical spectroscopy. Absorption spectra were collected in 2 mm cuvettes using TiN dispersed in ultrapure water using a Cary-50 spectrometer. The near-infrared spectral range was collected using the same samples on a Nicolet 6700 FT-IR.

Electron microscopy. Transmission electron microscopy (TEM) was performed using a JEOL-2000F microscope operated at 200 keV. Dilute samples were prepared by dropcasting on carbon-coated copper TEM grids.

Static Powder X-ray Diffraction. Temperature-dependent static X-ray diffraction was conducted at the Jerome B. Cohen X-ray Facility at Northwestern University on a 9 kW Cu rotating anode Rigaku SmartLab XE x-ray diffractometer using a Rigaku D/tex Ultra 250 HE 1D silicon strip detector for reduced data collection time. Nanocrystalline TiN powder was loaded onto a sample holder and then placed in an Anton Paar HTK1200N heating stage for measurement in θ/2θ reflection mode geometry. Measurements of static, temperature-dependent X-ray diffraction were performed using Cu K-α X-rays (1.54 Å). The sample was heated to 400 °C at a ramp rate of 10 °C/min. Measurements were collected every 25 °C up to 200 °C and every 50 °C thereafter. The sample was allowed to equilibrate for 10 minutes at each measurement temperature before diffraction was acquired.

Transient X-ray diffraction. Time-resolved x-ray diffraction was conducted at Beamline 11 ID-D of the Advanced Photon Source at Argonne National Laboratory. TiN NCs were dispersed in water and flowed as a 762 μm jet using a peristaltic pump. NCs were excited in an air-free interaction

region using the 400 nm, frequency-doubled output of a 1.6 ps Ti:sapphire laser operating at 10 kHz. NC structure was probed using 11.72 keV, 79 ps x-ray pulses. A CeO_2 film was used as a standard for *q* calibration. Powder x-ray diffraction patterns were collected using 20 s exposures on a time-gated Pilatus 2M detector and then azimuthally integrated. Individual scans were normalized to the average value in the baseline region between 3.1 and 4.0 $Å^{-1}$. Averaged scans were then differenced ($\Delta S = S_{pump\ on} - S_{pump\ off}$) to obtain transient X-ray diffraction data. For purposes of calculating the peak scattering intensity, raw scattering data was background corrected.

Temperature estimations as described in the text necessitate a defined photoexcited fraction, *f*, which is here defined as the fraction jet diameter (0.762 mm) which is exposed to a fraction of the initial intensity (I_0) of I_0/e^2, based upon the absorption spectra in Figure S8, using Beer's law. This definition of the photoexcited fraction arises from the necessity of concentrated sample loading to achieve appreciable signal in the transient diffraction measurements. As a result, excitation is inhomogeneous, as dictated by Beer's law. The close correspondence of integration (with *f* of 0.92 or 0.93) and derivative-type analysis (assuming *f*=1 in which all scattering contributes to ΔS) argues for the accuracy of the values of *f* assumed in the text.

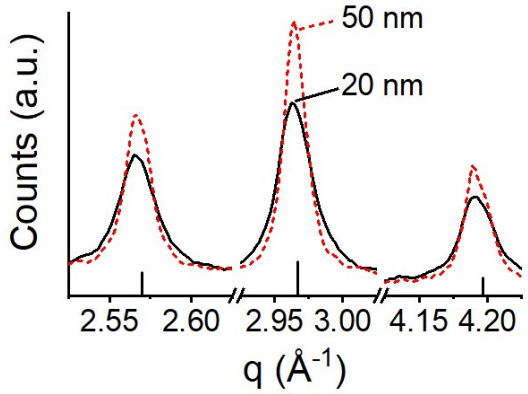

Figure S1. Selected range of room temperature powder X-ray diffraction data from 20 nm and 50 nm TiN nanoparticles. Solid lines indicate bulk TiN reflections.

Table S1. Crystallite size analysis of X-ray diffraction data**

Sample/Peak	Peak (2θ)	FWHM (2θ)	Crystallite Size (nm)
20 nm/ (111)	36.71	0.39	22.19
20 nm/ (200)	42.66	0.44	20.15
20 nm/ (220)	61.92	0.48	20.21
50 nm/ (111)	36.72	0.28	31.72
50 nm/ (200)	42.66	0.29	30.75
50 nm/ (220)	61.91	0.37	26.16

**Calculated according to the formula $s = K\lambda/\beta\cos\theta$, in which $K = 0.9$ and β is the full width at half maximum in radians, using Cu K-α X-rays.

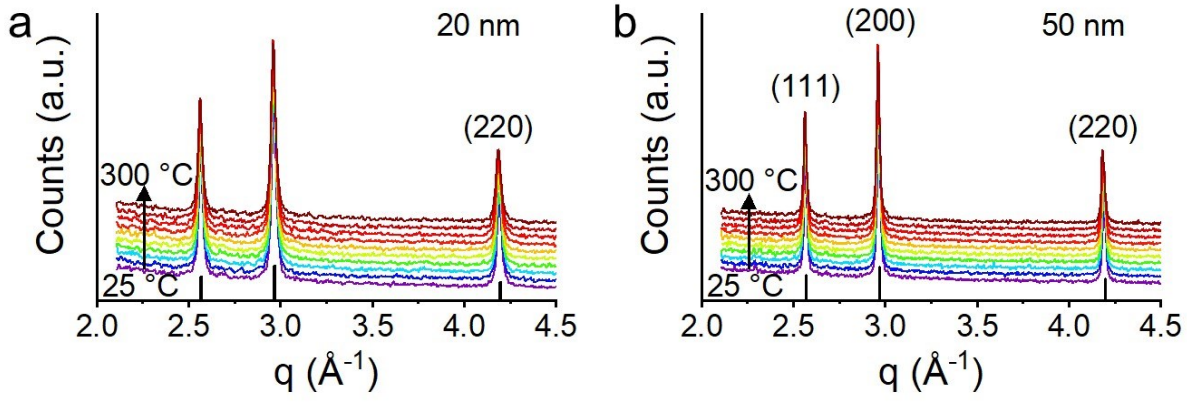

Figure S2. Full q-range of temperature-dependent powder X-ray diffraction data for (a) 20 nm and (b) 50 nm TiN nanoparticles.

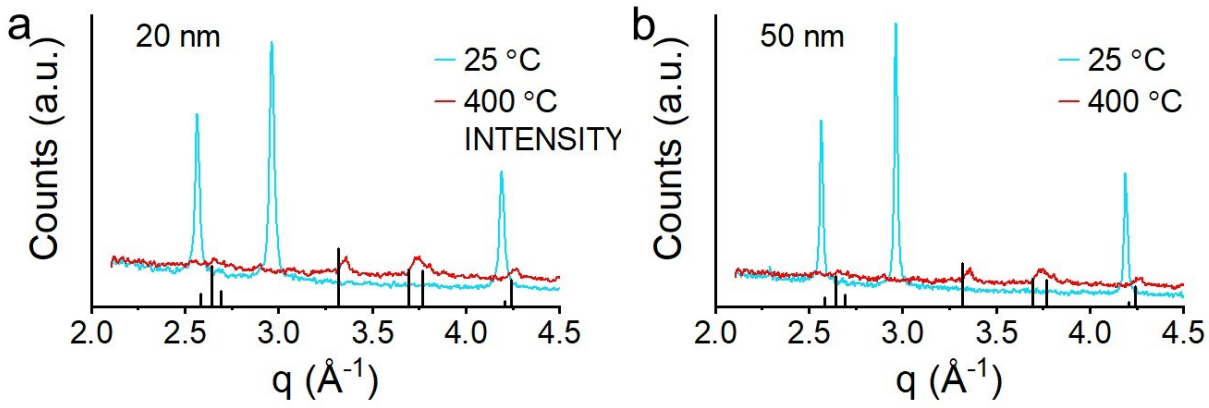

Figure S3. Powder X-ray diffraction data of (a) 20 nm and (b) 50 nm TiN NP powders at 25 °C and 400 °C. Black vertical lines represent diffraction of anatase phase TiO_2.

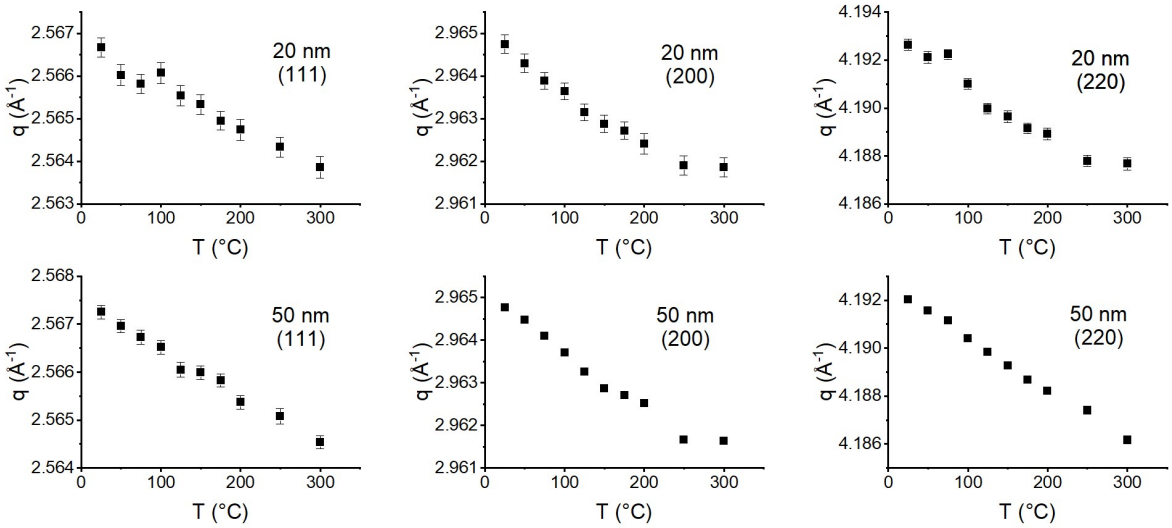

Figure S4. Fitted peak q values from static, temperature-dependent X-ray diffraction, for each nanoparticle size and reflection.

Table S2. Slope of $\Delta q_{hkl}/\Delta T$ for TiN nanoparticles

Sample/Peak	Peak Shift ($\times 10^{-5}$ Å^{-1}·°C^{-1})
20 nm/ (111)	-0.97±0.06
20 nm/ (200)	-1.10±0.08
20 nm/ (220)	-2.05±0.02
50 nm/ (111)	-0.98±0.03
50 nm/ (200)	-1.25±0.07
50 nm/ (220)	-2.15±0.04

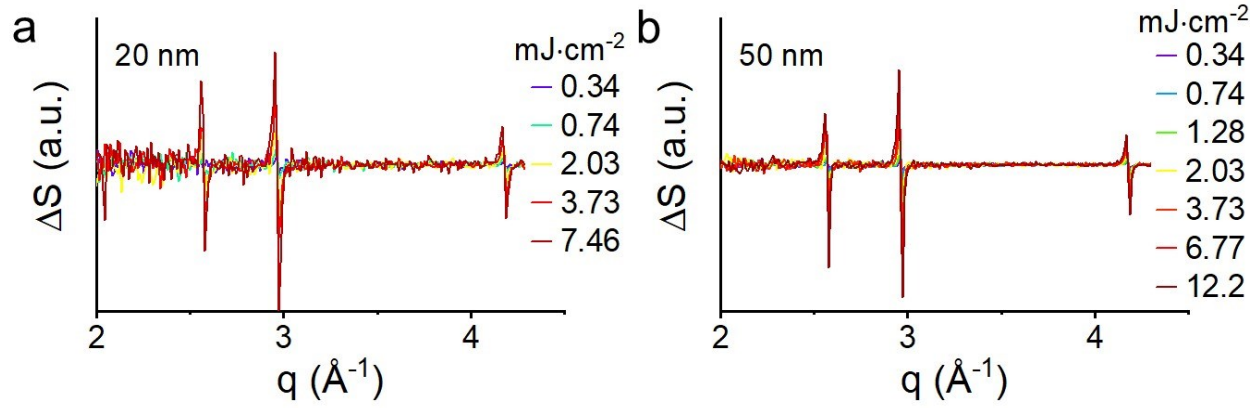

Figure S5. Full transient X-ray diffraction scattering pattern collected for various specified powers on (a) 20 nm and (b) 50 nm TiN nanoparticles.

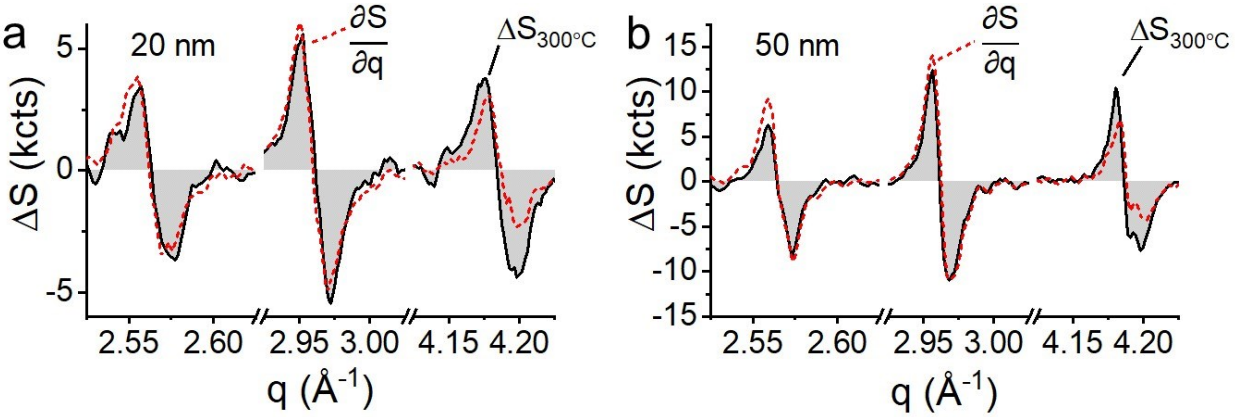

Figure S6. (a, b) Differenced diffraction data, ΔS_{300} = S_{300} - S_{25}, of (a) 20 nm TiN nanoparticles and (b) 50 nm TiN nanoparticles shown in black. The dashed red curves are the first derivatives of X-ray scattering data collected at 25 °C multiplied by Δq of -0.003.

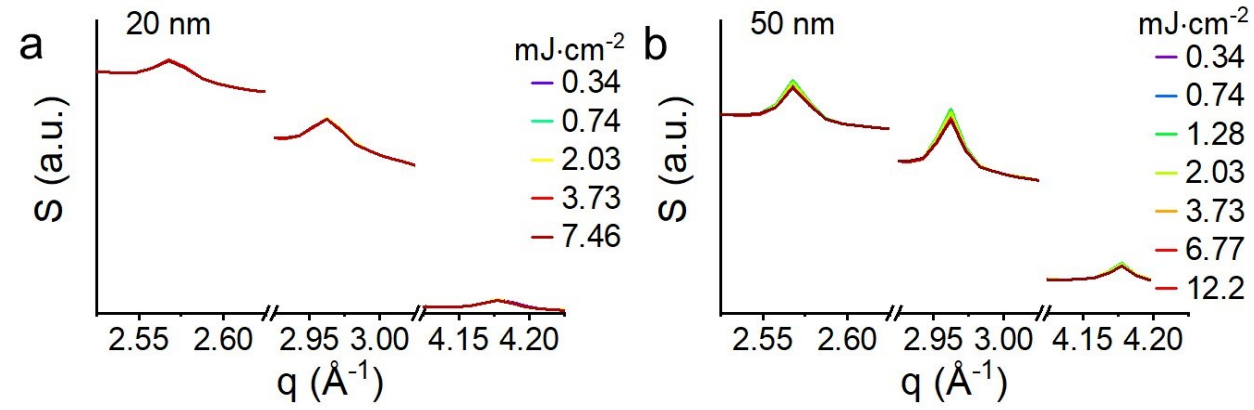

Figure S7. Selected raw transient X-ray scattering powder diffraction patterns without background correction for (a) 20 nm and (b) 50 nm TiN nanoparticles.

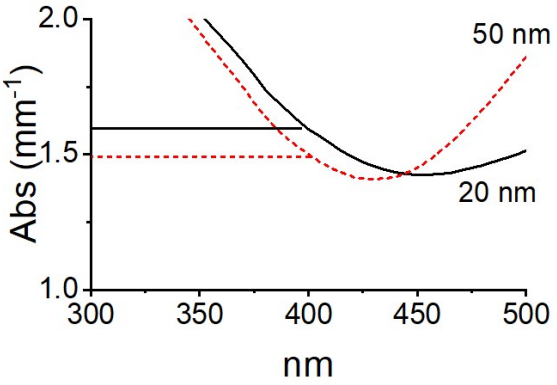

Figure S8. Extinction per millimeter of TiN NP solutions. Approximately 90 percent of pump light is absorbed in the jet used experimentally. Tie lines show the absorption of the samples at the 400 nm pump photon wavelength. The 20 nm sample absorbs approximately 94 % of incident 400 nm pump light along the diameter; the 50 nm sample absorbed approximately 93 % of the incident 400 nm pump light along the diameter.

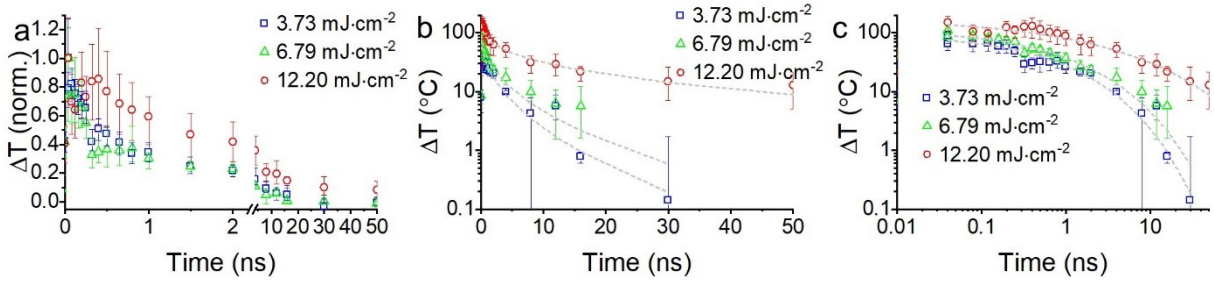

Figure S9. (a) Normalized temperature dynamics of 50 nm TiN NPs under different 400 nm pump fluence conditions specified in the caption. Temperatures are estimated as described in the text with errors bars representing high and low estimates from (111), (200), and (220) peaks, with data normalized to the peak change in temperature for each of the measurements. (b) Semi-log plot of temperature dynamics of 50 nm TiN NPs under 400 nm pump excitation. (c) Log-log plot of the same data.